Physics of Wave Processes and Radio Systems
2025, vol. 28, no. 1, pp. 39–55

DOI 10.18469/1810-3189.2025.28.1.39-55
UDC 621.372.543.2
Original Research

Received 4 November 2024
Accepted 5 December 2024
Published 31 March 2025

Methods of designing bandpass filters on coupled coaxial resonators

Yurii G. Belov, Vladimir V. Biryukov, Ilya A. Vorobyov, Vasiliy A. Malakhov, Aleksey S. Raevskiy, Yuliya V. Raevskaya

Nizhny Novgorod State Technical University named after R.E. Alekseev
24, Minin Street,
Nizhny Novgorod, 603950, Russia

Abstract – **Background.** Ultrahigh frequency bandpass filters are widely used in various radio engineering devices. A special place among microwave band-pass filters is occupied by filters that are part of multiplexers, in particular, diplexers used in cellular communication systems. Filter and diplexer designs based on coaxial resonators are widely used in mobile communication systems. Filters on coaxial resonators have a fairly well-developed design and can be used for broadband systems. **Aim.** Currently, the design of filters and diplexers on coaxial resonators continues to be improved in terms of manufacturing and assembly technology. **Methods.** The method of equivalent circuits, communication matrices. **Results.** The principles of constructing filters on coupled coaxial resonators are considered. The methods of obtaining a given shape of the amplitude-frequency response of the filter are analysed. **Conclusion.** A method for designing transfer functions and synthesising prototypes of filter circuits with Chebyshev characteristics is considered.

Keywords – bandpass filters; coaxial resonator; amplitude-frequency response; coupling matrix.

Introduction

Ultra-high frequency bandpass filters (BPF) [1; 2] are widely used in various radio engineering devices. The general theory of UHF BPF is fairly fully described in [3]. Filters that are part of multiplexers, in particular diplexers used in cellular communication systems, occupy a special place among UHF BPFs. Filter and diplexer designs based on coaxial resonators [4; 5] are widely used in mobile communication systems. Filters based on coaxial resonators have a well-established design and can be used for broadband systems. Currently, the design of filters and diplexers based on coaxial resonators is being improved in terms of manufacturing and assembly technology.

Crosstalk in coaxial bandpass filters

The receive and transmit bandpass filters that are part of base station diplexers can have the required attenuation levels of more than 100 dB on one side of the passband and at the same time have very mild attenuation requirements on the opposite side [6].

The cross-coupling method is widely used to create asymmetric frequency characteristics, as it allows suppression in the filter only in the frequency band where it is necessary. Using the cross-coupling method to create transmission zeros, it is possible to increase suppression above the passband and weaken suppression below the passband. This reduces the number of resonant elements required to meet the requirements, which in turn reduces the losses, size and cost of manufacturing the filter design, albeit at the expense of topological complexity and, possibly, development and tuning time. The total coupling between adjacent resonators has both magnetic and electrical components, but they are not in phase with each other, so the total coupling is the magnetic coupling minus the electrical coupling [7]. For this reason, the tuning screw placed between the open ends of two resonators increases the coupling between them. The non-resonant (outside the passband) behaviour of the elements is used to create destructive interference, resulting in zero transmission.

Multipath connection diagrams

Consider the three-resonator structure shown in Fig. 1, which is a cascade-triplet section using inductive cross-coupling between resonators 1 and 3. The resonators of the equivalent circuit are shown as circles. Phase shifts can be found for two possible signal paths. Path 1–2–3 is the main path, and path 1–3 is the secondary path following the cross-coupling. When summing the phase contributions of the individual components, the contributions of resonators 1 and 3 are not required, as both paths have a common start and end. Only the contribution of the internal elements of the circuit to resonators 1 and 3 needs to be

✉ raevsky_as@mail.ru (*Alexey S. Raevsky*)

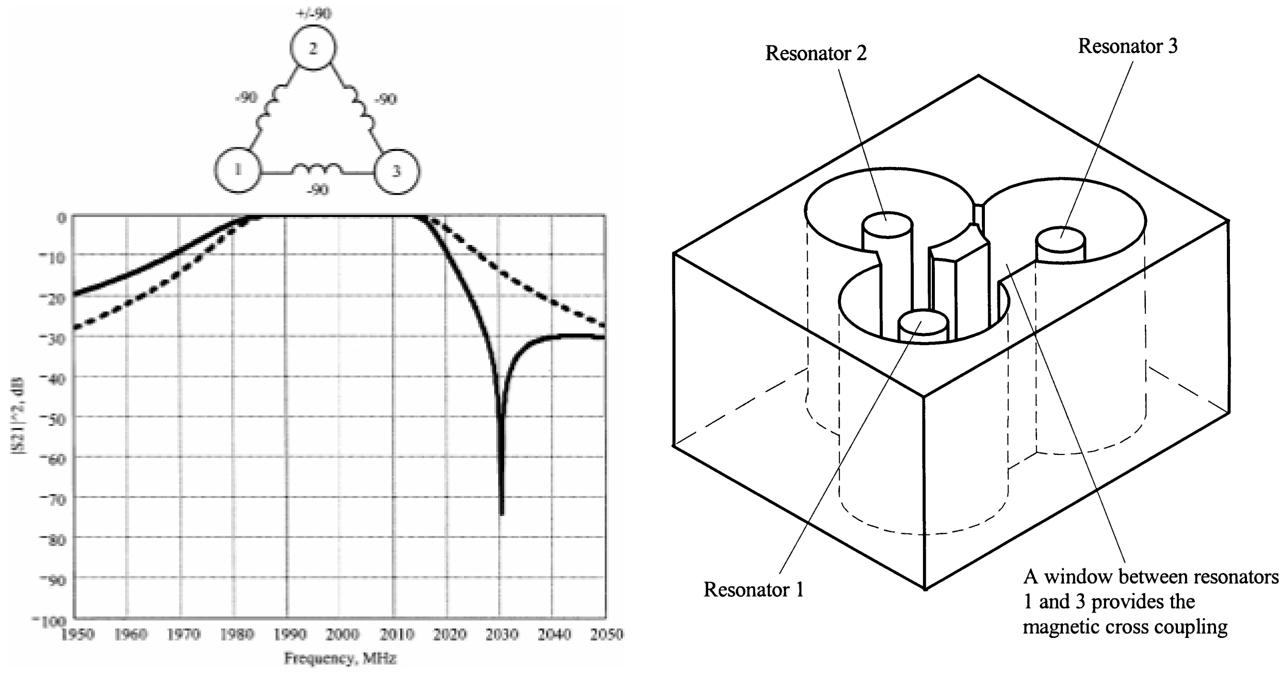

a *b*

Fig. 1. Multipath diagram for a cascade-triplet section with inductive cross-coupling and possible frequency response, including transmission zero (solid line) (a) and a physical representation of the section of the cascade-triplet section (b)

Рис. 1. Диаграмма многолучевой связи для каскадно-триплетной секции с индуктивной перекрестной связью и возможной частотной характеристикой, включая нуль передачи (сплошная линия) (*а*) и физическое представление сечения каскадно-триплетной секции (*б*)

taken into account. Indeed, 1 and 3 do not even have to be resonators; the signals can be combined at the input or output of the filter itself. In addition, resonator 2 should be considered both above and below resonance.

The window between resonators 1 and 3 provides magnetic cross-coupling. Below resonance, the two paths are in phase, and above resonance, the two paths are 180° out of phase. This is only accurate at one frequency (here approximately 2030 MHz), but it is approximately accurate for frequencies around 2020–2040 MHz.

This destructive interference causes a transmission zero to appear at the upper edge of the passband. A stronger coupling between resonators 1 and 3 causes the zero to move towards the passband. Decreasing the coupling moves it further along the upper edge. This type of cross-coupling can be implemented by a window between the cavities in the same way as the primary coupling between resonators 1 and 2 or between 2 and 3. Its advantage is that no additional components are required, Fig. 1, *b*.

In Fig. 2, *a*, the inductive coupling between resonators 1 and 3 is replaced by a capacitive probe. Again, path 1–2–3 is the main path. Path 1–3 is the secondary path and now has a positive phase shift of 90°. Thus, for capacitive cross-coupling, destructive interference occurs below the passband.

Fig. 2, *b* shows a variant with four resonators, known as a cascaded quadruplet section with inductive cross-coupling. The primary path in this case is 1–2–3–4, and the secondary path is 1–4, thus bypassing two resonators. No transmission zeros are formed at any real frequencies above or below the passband. However, zeros can form at imaginary frequencies, which leads to smoothing of the group delay in the passband.

Smoothing the group delay also leads to smoothing the introduced losses. Losses in the middle band increase slightly, while the effects of the decline at the edges of the band decrease. These effects are not obvious from this analysis; a more detailed analysis of filters with transmission zeros at imaginary frequencies is given in [8; 9].

Replacing the inductive element between resonators 1 and 4 with a capacitive probe results in a different type of cascade-quadruplet section. This topology is particularly interesting because transmission zeros are formed both above and below the passband (Fig. 3). The probe between resonators 1 and 4 provides a capacitive coupling.

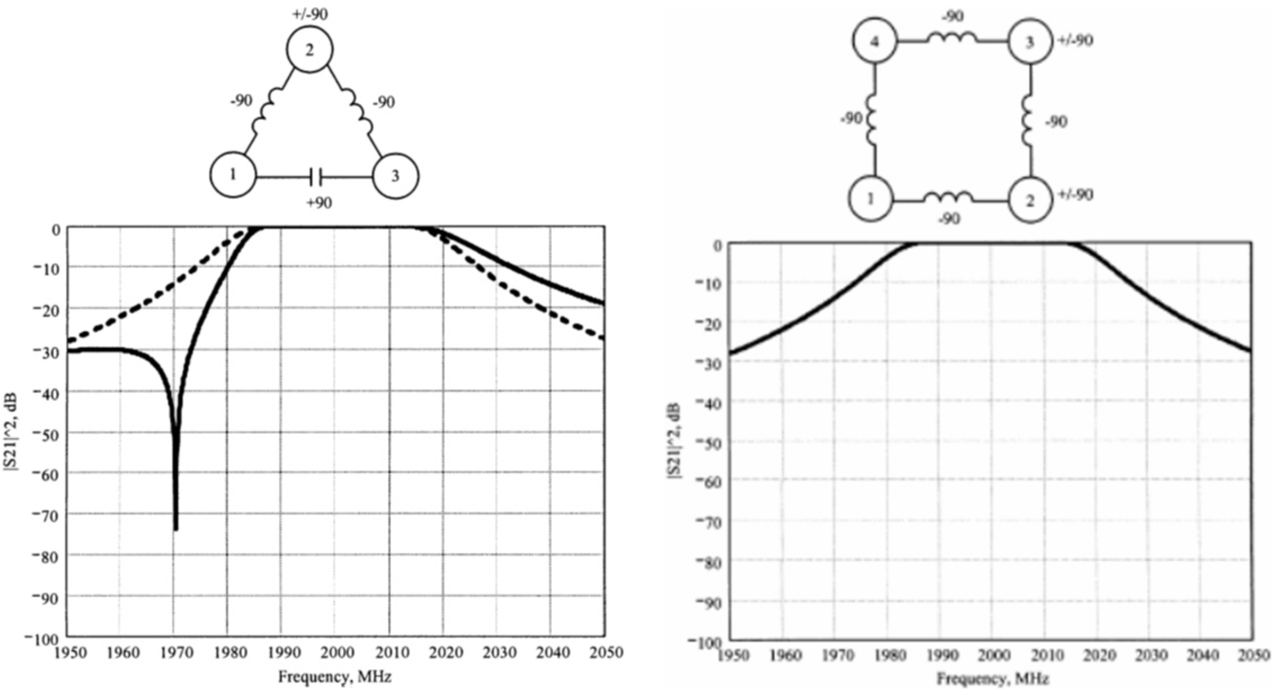

a *b*

Fig. 2. Multipath diagram and possible frequency response for cascade-triplet section with capacitive cross coupling (including transmission zero – solid line, standard Chebyshev response without cross coupling – dotted line) (*a*) and for cascade-quadruplet section with inductive cross coupling (*b*)

Рис. 2. Диаграмма многолучевой связи и возможная частотная характеристика для каскадно-триплетной секции с емкостной перекрестной связью (включая нуль передачи – сплошная линия, стандартный отклик Чебышева без перекрестной связи – пунктирная линия) (*a*) и для каскадно-квадруплетной секции с индуктивной перекрестной связью (*б*)

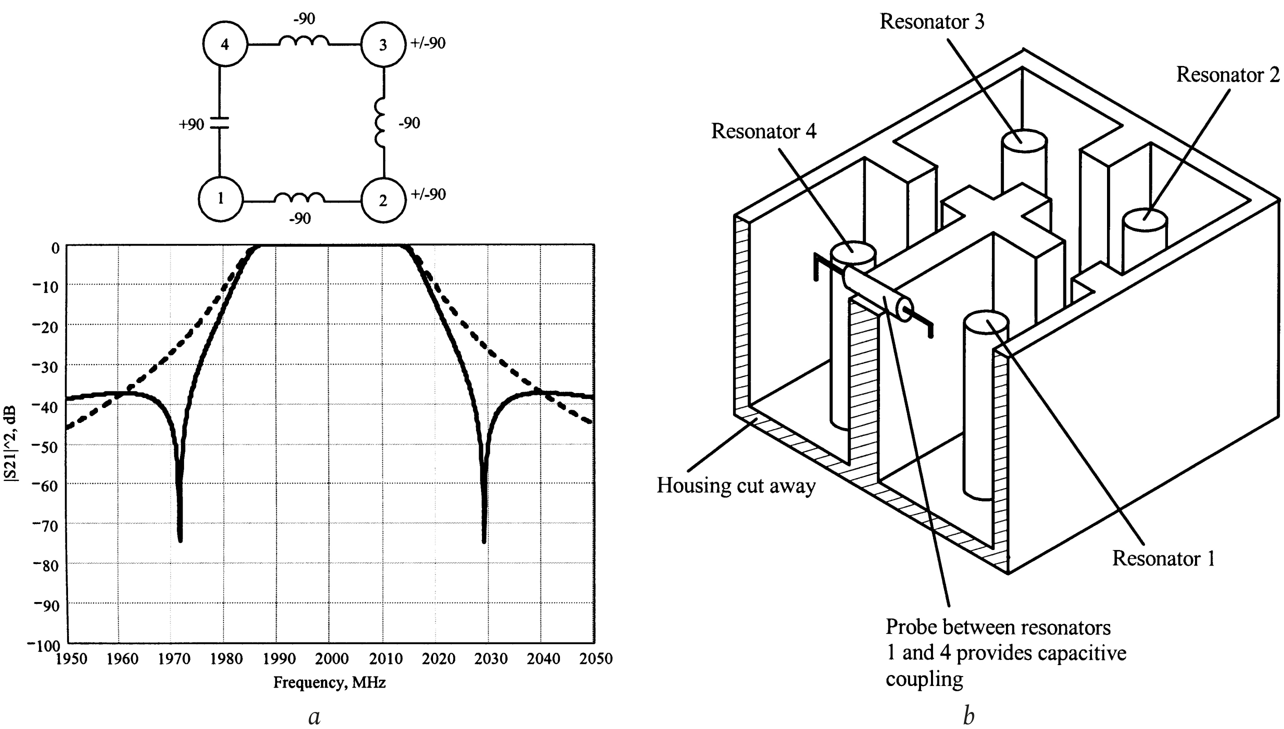

a *b*

Fig. 3. Multipath diagram for cascade-quadruplet section with capacitive cross-coupling and possible frequency response (*a*); physical representation of the section of cascade-quadruplet section (*b*)

Рис. 3. Диаграмма многолучевой связи для каскадно-квадруплетной секции с емкостной перекрестной связью и возможная частотная характеристика (*a*); физическое представление сечения каскадно-квадруплетной секции (*б*)

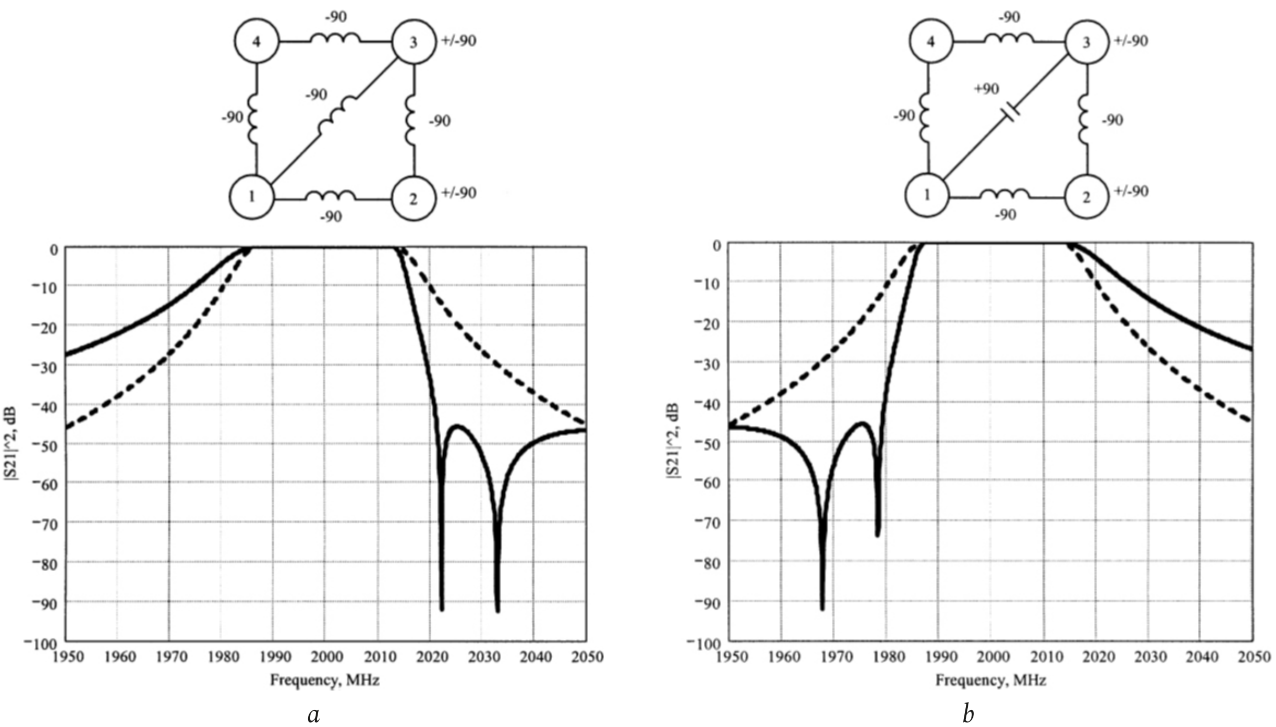

Fig. 4. Nested cross-linking to obtain two transmission zeros at the upper (*a*) and lower (*b*) edge of the bandwidth (solid line)
Рис. 4. Вложенная перекрестная связь для получения двух нулей передачи на верхнем (*а*) и нижнем (*б*) крае полосы пропускания (сплошная линия)

Nested structures

Let us examine nested structures with three or more signal paths. First, consider the diagram in Fig. 4, *a*. The outer path 1–2–3 combines with 1–3 to form a single transmission zero. Simultaneously, the internal path 1–3–4 combines with the innermost path 1–4 to create a second transmission zero. Both zeros are located at the upper edge of the passband. It has been shown that two signal paths can be combined to produce a transmission zero.

Similarly, the circuit in Fig. 4 *b* provides two transmission zeros at the lower edge of the passband. Its distinctive feature is the capacitive coupling between resonators 1 and 3. These two circuits are particularly useful in diplexer designs due to their similar topology and response symmetry.

[10] provides an overview of the use of coupling between non-adjacent resonators to create transmission zeros at real frequencies in microwave filters. Multipath connections are considered, diagrams and relative phase shifts of multiple observed paths causing known responses of cascade triple and quadruple sections are constructed. A brief classification of various methods for synthesising and implementing these types of filters is given.

1. Determination of the Required Orders

The transfer function of a two-port filter circuit is a mathematical description of the circuit's response, namely a mathematical expression of the filter's transfer coefficient as a four-pole S_{21}. In many cases, the square of the transfer function modulus for a passive filter without losses is defined as

$$\left|S_{21}\left(j\Omega\right)\right|^2 = \frac{1}{1+\varepsilon^2 F_n^2\left(\Omega\right)}, \tag{1}$$

where ε is the ripple constant; $F_n(\Omega)$ is the filter or characteristic function; Ω is the frequency variable. It is usually convenient to represent the frequency variable as the frequency of the low-frequency prototype filter, which has a cutoff frequency Ω_c, = 1 (rad/s). For linear stationary circuits, the transfer function can be defined as a rational function, i.e.

$$S_{21}\left(p\right) = \frac{N(p)}{D(p)}, \tag{2}$$

where *N*(*p*) and *D*(*p*) *are* polynomials of the complex frequency variable ρ = σ + jω. For a passive circuit without losses, the real part of the complex variable frequency σ = 0 and *p* = jω. The search for a realizable rational transfer function that gives response characteristics approximating the required response is the so-called approximation problem, and in many cases the rational transfer function (2) can be constructed

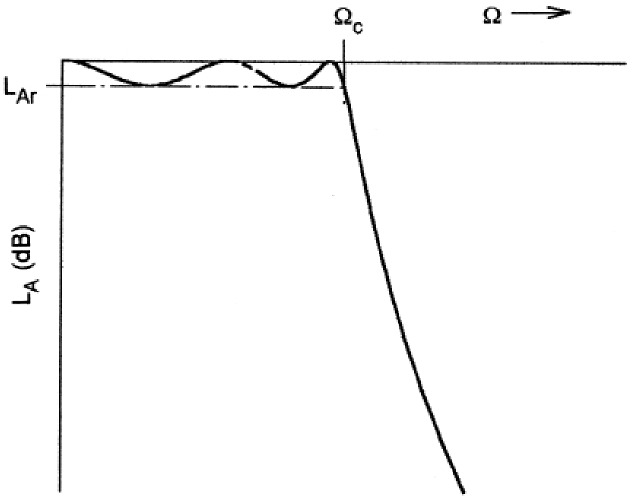

Fig. 5. Chebyshev characteristic of filter transmission
Рис. 5. Чебышевская характеристика передачи фильтра

from the square of the modulus of the transfer function (1) [11; 12].

For a given transfer function (1), the characteristic of the filter losses, corresponding to the generally accepted definition, can be calculated using the formula

$$L_A(\Omega) = 10\log\frac{1}{\left|S_{21}(j\Omega)\right|^2}, \text{ dB}. \quad (3)$$

Since for a passive two-port circuit without losses $\left|S_{11}\right|^2 + \left|S_{21}\right|^2 = 1$, the value of the filter's reverse losses can be found using the expression

$$L_R(\Omega) = 10\log\left(1-\left|S_{21}(j\Omega)\right|^2\right), \text{ дБ}. \quad (4)$$

The plane (σ,Ω) on which the rational transfer function is defined is called the complex plane, or p-plane. The horizontal axis of this plane is called the real axis, or a-axis, and the vertical axis is called the imaginary axis, or jΩ-axis. The values of p at which the function becomes zero are the zeros of the function, and the values of p at which the function becomes infinite are the singularities (usually poles) of the function. Consequently, the zeros of S_{21} (p) are the roots of the numerator $N(p)$, and the poles of S_{21} (p) are the roots of the denominator $D(p)$.

These poles are the natural frequencies of the filter, whose response is described by S_{21} (p). For the filter to be stable, these natural frequencies must lie in the left half of the p-plane or on the imaginary axis.

Consequently, $D(p)$ is a Hurwitz polynomial [13], i.e. its roots (or zeros) are located within the left half-plane or on the jΩ axis, while the roots (or zeros) *of* $N(p)$ can be located anywhere on the entire complex plane. The zeros of $N(p)$ are called the zeros of the filter transmission.

The poles and zeros of a rational transfer function can be plotted on *the p-plane*. Different types of transfer functions differ in the position of zeros and poles on the diagram.

The Chebyshev function, which provides a passband with equal ripple and a stopband with the smoothest amplitude response, is shown in Fig. 5.

The square of the transfer function describing this type of response has the form

$$\left|S_{21}(j\Omega)\right|^2 = \frac{1}{1+\varepsilon^2 T_n^2(\Omega)}, \quad (5)$$

where the ripple constant e is related to the specified ripple value of the passband L_{Ar} in dB by the relationship

$$\varepsilon = \sqrt{10^{\frac{L_{A_r}}{10}} - 1}, \quad (6)$$

and T_n (Ω) is a Chebyshev function of the first kind of order n.

Rhodes [12] derived a general formula for the rational transfer function for a Chebyshev filter:

$$S_{21}(p) = \frac{\prod_{i=1}^{n}\sqrt{\eta^2+\sin^2\left(\frac{i\pi}{n}\right)}}{\prod_{i=1}^{n}\left(p+p_i\right)}, \quad (7)$$

where

$$\eta = \operatorname{sh}\left(\frac{1}{n}\operatorname{arcsh}\left(\frac{1}{\varepsilon}\right)\right), \quad (8)$$

$$p_i = j\cos\left(\arcsin(j\eta)+\frac{(2i-1)\pi}{2n}\right).$$

All zeros of the transfer function $S_{21}(p)$ are located at infinity. Therefore, Chebyshev filters are sometimes called full-pole filters. In the case of a Chebyshev filter, the poles lie on an ellipse in the left half-plane of the complex frequency. The major axis of the ellipse is located on the jΩ axis and is equal to $\sqrt{1+\eta^2}$, while the minor axis is located on the σ axis and has a size of η. The synthesis of filters for implementing such transfer functions leads to the creation of so-called low-pass filter prototypes [13–15].

A low-pass filter prototype is generally defined as a low-pass filter whose element values are normalised such that the source resistance or conductance is equal to unity, denoted by $g_0 = 1$, and the angular cutoff frequency is equal to unity, denoted by $\Omega_c = 1$ (rad/s). For example, Fig. 6 shows two possible forms of a n-pole low-pass filter prototype for implementing the pole characteristic of the filter, includ-

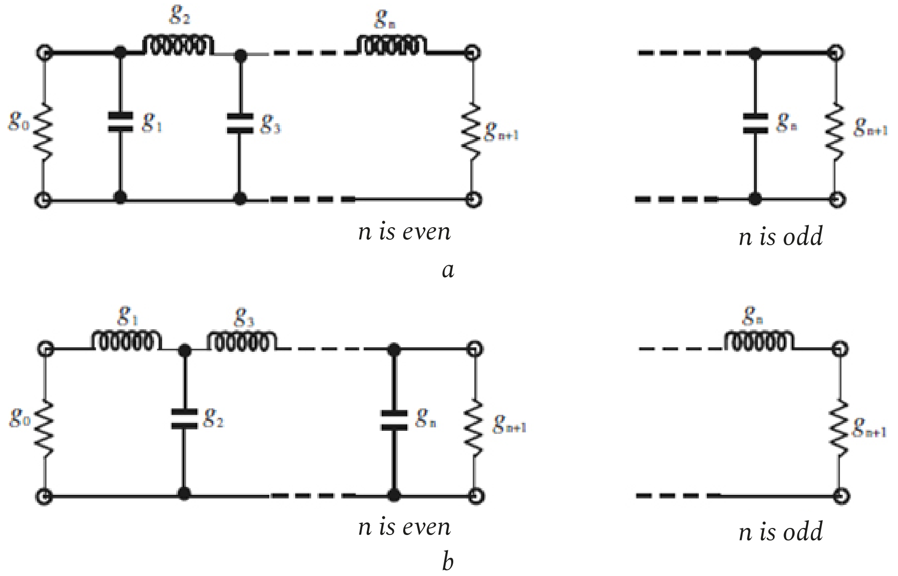

Fig. 6. Prototypes of the n-pole low-pass filter
Рис. 6. Прототипы *n*-полюсного фильтра нижних частот

ing Butterworth, Chebyshev, and Gaussian characteristics. Any of the forms can be used, as they give the same response. It should be noted that in Fig. 6, g_i for values of i from 1 to n represents either the inductance of the series inductance coil or the capacitance of the shunt capacitor.

Therefore, n is the number of reactive elements. If g_1 is the shunt capacitance or series inductance, then g_0 is defined as the source resistance or source conductance. Similarly, if g_n is the shunt capacitance or series inductance, then g_{n+1} is the load resistance or load conductance. Unless otherwise specified, these g values are assumed to be inductance in henries, capacitance in farads, resistance in ohms, and conductance in siemens.

This type of low-pass filter can serve as a prototype for the design of many practical filters. For an acceptable ripple value in the passband L_{Ar}, dB, minimum attenuation in the stopband L_{As}, dB at $\Omega = \Omega_s$, the degree of the Chebyshev low-pass device prototype that will meet these requirements can be determined using the expression

$$n \geq \frac{\operatorname{arcch}\left(\sqrt{\dfrac{10^{0,1L_{A_s}}-1}{10^{0,1L_{A_r}}-1}}\right)}{\operatorname{arcch}(\Omega_s)}. \tag{9}$$

Sometimes, instead of the ripple level value in the passband $L_{(Ar)}$, the minimum reverse loss value L_R or the maximum value of the voltage standing wave ratio SWR in the passband is specified.

These values are related by the following equations:

$$L_{A_r} = -10\log\left(1-10^{0,1L_R}\right),\ \text{дБ}. \tag{10}$$

$$\text{КСВН} = \frac{1+|S_{11}|}{1-|S_{11}|}. \tag{11}$$

$$L_{A_r} = -10\log\left(1-\left(\frac{\text{КСВН}-1}{\text{КСВН}+1}\right)^2\right),\ \text{дБ}. \tag{12}$$

The characteristic of the prototype LPF can be converted to the characteristic of the PPF with a passband $\omega_2 - \omega_1$, where ω_1 and ω_2 denote the angular frequencies at the passband boundary. The required frequency conversion is performed as follows:

$$\Omega = \frac{\Omega_c}{FBW}\left(\frac{\omega}{\omega_0}-\frac{\omega_0}{\omega}\right), \tag{13}$$

where

$$FBW = \frac{\omega_2-\omega_1}{\omega_0}, \tag{14}$$

$$\omega_0 = \sqrt{\omega_1\omega_2}. \tag{15}$$

Applying this frequency conversion to the parallel capacitor C and series inductance L of the prototype low-pass filter, we have

$$j\omega C \to j\omega\frac{\omega_c C}{FBW\omega_0} + \frac{1}{j\omega\dfrac{FBW}{\omega_c\omega_0 C}}; \tag{16}$$

$$j\omega L \to j\omega\frac{\omega_c L}{FBW\omega_0} + \frac{1}{j\omega\dfrac{FBW}{\omega_c\omega_0 L}},$$

This means that the parallel capacitor C or series inductance L in the low-frequency prototype is converted into a parallel or series LC resonant circuit.

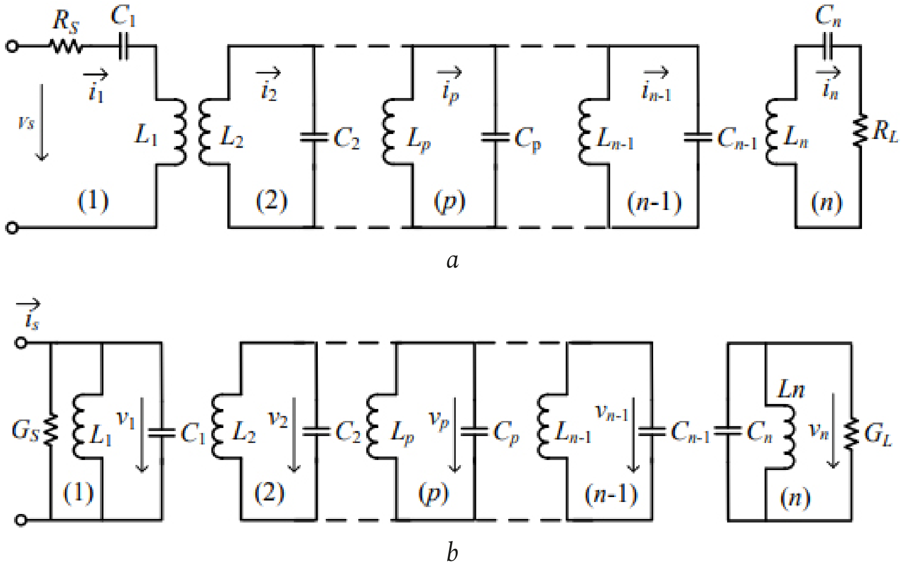

Fig. 7. Equivalent filter circuit of n-coupled resonators for the contour current method (*a*) and the nodal potential method (*b*)
Рис. 7. Эквивалентная схема фильтра из *n*-связанных резонаторов для метода контурных токов (*а*) и метода узловых потенциалов (*б*)

2. Obtaining Filter Coupling Matrices

A chain of coupled resonators can be converted into a matrix form called a coupling matrix. The theory of the coupling matrix has advantages in the application of matrix operations, such as matrix rotation (similarity transformation) and matrix inversion, in circuit design. Topology reconfiguration and circuit synthesis are simplified by such matrix operations [16–18].

The theory of coupling matrices is only suitable for narrowband filter circuits, since it is based on the assumption of frequency independence of the transfer coefficients of inverters.

Coupling matrices can be divided into two categories. The first is a general $p \times p$ coupling matrix, where p is the order of the circuit. The other category, including the $p+2$ coupling matrix, has additional columns and rows for ports.

In the early 1970s, Atiya and Williams [19–22] first introduced a method for designing a bandpass waveguide filter based on a coupling matrix. They used a $p \times p$ coupling matrix as the matrix.

The filter is a p-order cascade filter connected by transformers or magnetic links. Each resonator has a capacitor C = 1 F and an inductance coil L = 1 H. Thus, all resonators resonate at a frequency of 1 Hz. R_s and R_L are the source and load resistances (the equivalent unit circuit is assumed to be lossless, with resistance or conductivity existing only in the source and load); i is the circuit current of each resonator. The connection between resonators p and q is denoted as $M_{p,q}$, it is a real number and frequency independent.

The coupling matrix theory can be extended to circuits with asynchronously tuned resonators or to a general $n \times n$ coupling matrix. The formulation of the general $n \times n$ coupling matrix is considered in [11]. Filters with magnetically and electrically coupled resonators are considered separately.

An equivalent circuit with magnetically coupled resonators is shown in Fig. 7, *a*. Using Kirchhoff's rules, the coupling matrix is obtained from the impedance matrix from the system of equations for loop currents. Another circuit with electrical coupling is shown in Fig. 7, *b*. The coupling matrix is determined from the admittance matrix, formulated using the system of equations for node potentials. Regardless of the type of coupling, the general matrix [*A*], composed of the coupling coefficients $t_{p,q}$ and external quality factors q_{ei}, is presented in [9] as

$$\left[\mathbf{A}\right] = \left[\mathbf{Q}\right] + p\left[\mathbf{U}\right] + j\left[\mathbf{m}\right], \tag{17}$$

where

$$p = j\frac{1}{FBW}\left(\frac{\omega}{\omega_0} - \frac{\omega_0}{\omega}\right), \tag{18}$$

$$\left[\mathbf{Q}\right] = \begin{bmatrix} \frac{1}{q_{e1}} & 0 & \dots & 0 \\ 0 & 0 & \dots & 0 \\ \dots & \dots & \dots & \dots \\ 0 & 0 & \dots & \frac{1}{q_{en}} \end{bmatrix}, \tag{19}$$

$$\left[\mathbf{m}\right] = \begin{bmatrix} m_{1,1} & m_{1,2} & \dots & m_{1,n} \\ m_{2,1} & m_{2,2} & \dots & m_{2,n} \\ \dots & \dots & \dots & \dots \\ m_{n,1} & m_{n,2} & \dots & m_{n,n} \end{bmatrix}. \tag{20}$$

$$[m]_{(n+2)\times(n+2)} = \begin{bmatrix} m_{s,s} & m_{s,1} & \cdots & m_{s,n-1} & m_{s,n} & m_{s,l} \\ m_{1,s} & m_{1,1} & \cdots & m_{1,n-1} & m_{1,n} & m_{1,l} \\ \vdots & \vdots & \ddots & \vdots & \vdots & \vdots \\ m_{n-1,s} & m_{n-1,1} & \cdots & m_{n-1,n-1} & m_{n-1,n} & m_{n-1,l} \\ m_{n,s} & m_{n,1} & \cdots & m_{n,n-1} & m_{n,n} & m_{n,l} \\ m_{l,s} & m_{l,1} & \cdots & m_{l,n-1} & m_{l,n} & m_{l,l} \end{bmatrix}_{(n+2)\times(n+2)}$$

General n × n connection matrix

n + 2 connection matrix

Fig. 8. *n* + 2 coupling matrix
Рис. 8. Матрица связи *n* + 2

Matrix $[U]$ – unit matrix $n \times n$; p – complex variable frequency of low-frequency prototype; ω_0 – centre frequency of filter; FBW – relative filter bandwidth; q_{ei} ($i = 1$ and n) – normalised external Q factors of resonator i; $m_{p,q}$ ($p \neq q$) – normalised coupling coefficients between resonators p and q. They have the form

$$q_{ei} = Q_{ei} \cdot FBW; \quad m_{p,q} = \frac{M_{p,q}}{FBW}, \tag{21}$$

where Q_{ei} is defined as the external quality factor of resonator i; $M_{p,q}$ is defined as the coupling coefficient between resonators p and q; $m_{i,i}$ is the self-coupling of resonator i. The filter is asynchronously tuned if some of $m_{i,i}$ are non-zero elements.

As indicated in [20], the S-parameters of the filter can be calculated using the normalised external Q-factors q_{ei} and the matrix $[A]$ as

$$S_{11} = 1 - \frac{2}{q_{e1}}\left[\mathbf{A}\right]^{-1}_{1,1}; \tag{22}$$

$$S_{21} = \frac{2}{\sqrt{q_{e1} q_{en}}}\left[\mathbf{A}\right]^{-1}_{n,1}. \tag{23}$$

n + 2 and n + X coupling matrix

Extended from the general $n \times n$ coupling matrix, the $n + 2$ coupling matrix is used to describe a two-port circuit [23]. The general $n + 2$ coupling matrix is shown in Fig. 8.

The subscripts s and l denote the source and load, respectively. Compared to the general $n \times n$ connection matrix, the $n + 2$ connection matrix has additional columns and rows for the source and load surrounding the general $n \times n$ connection matrix. $m_{s,i}$ and $m_{i,s}$ describe the connection between the source and resonator i; $m_{l,i}$ and $m_{i,l}$ describe the connection between the load and resonator i; $m_{s,s}$ and $m_{l,l}$ – self-connection of the source and load. Thanks to the additional columns and rows of ports, the $n + 2$ connection matrix has a number of advantages.

One port can be connected to several resonators, and one resonator can be connected to several ports. The connection between the source and the load is possible in such a way as to provide a completely canonical filtering function (i.e., the number of transfer zeros at the end frequencies is equal to the number of resonators n). Thus, the $n + 2$ connection matrix is more general than the $n \times n$ connection matrix. In addition, the $n + 2$ connection matrix can be extended to a multi-port matrix, such as an $n + X$ connection matrix, which allows it to be used to describe not only filters but also multiplexers.

3. Synthesis of the Coupling Matrix

For filters with standard characteristics based on the found values of the prototype LPF $g_{(i)}$, the coupling coefficient $M_{i,i+1}$ and the external Q factor Q_{ei}- are determined directly [11] as

$$Q_{e1} = \frac{g_0 g_1}{FBW}, \quad Q_{en} = \frac{g_n g_{n+1}}{FBW}; \tag{24}$$

$$M_{i,i+1} = \frac{FBW}{\sqrt{g_i g_{i+1}}}, \quad i = 1, 2, \ldots, n-1. \tag{25}$$

The corresponding normalised values are as follows

$$q_{e1} = Q_{e1} \cdot FBW = g_0 g_1, \tag{26}$$

$$q_{en} = Q_{en} \cdot FBW = g_n g_{n+1};$$

$$m_{i,i+1} = \frac{M_{i,i+1}}{FBW} = \frac{1}{\sqrt{g_i g_{i+1}}}, \quad i = 1, 2, \ldots, n-1. \tag{27}$$

However, for filters with arbitrary characteristics, there is no simple solution. Usually, two methods are used to solve this problem. One is based on recursive methods and matrix rotation, the other on optimisation.

Synthesis method using matrix rotation

The synthesis of complex filters with transfer zeros was generalised by Cameron [23] and divided into three stages:

(1) A recursive method for obtaining polynomials that represent transmission and reflection characteristics.

$$M(7) = \begin{pmatrix} 0 & 0.866 & 0 & 0 & 0 & 0 & 0 \\ 0.866 & 0 & 0.611 & 0 & 0 & 0 & 0 \\ 0 & 0.611 & 0 & 0.572 & 0 & 0 & 0 \\ 0 & 0 & 0.572 & 0 & 0.572 & 0 & 0 \\ 0 & 0 & 0 & 0.572 & 0 & 0.611 & 0 \\ 0 & 0 & 0 & 0 & 0.611 & 0 & 0.866 \\ 0 & 0 & 0 & 0 & 0 & 0.866 & 0 \end{pmatrix}$$

$qe1(7) = 0.933$ $\qquad$ $qe2(7) = 0.933$

a

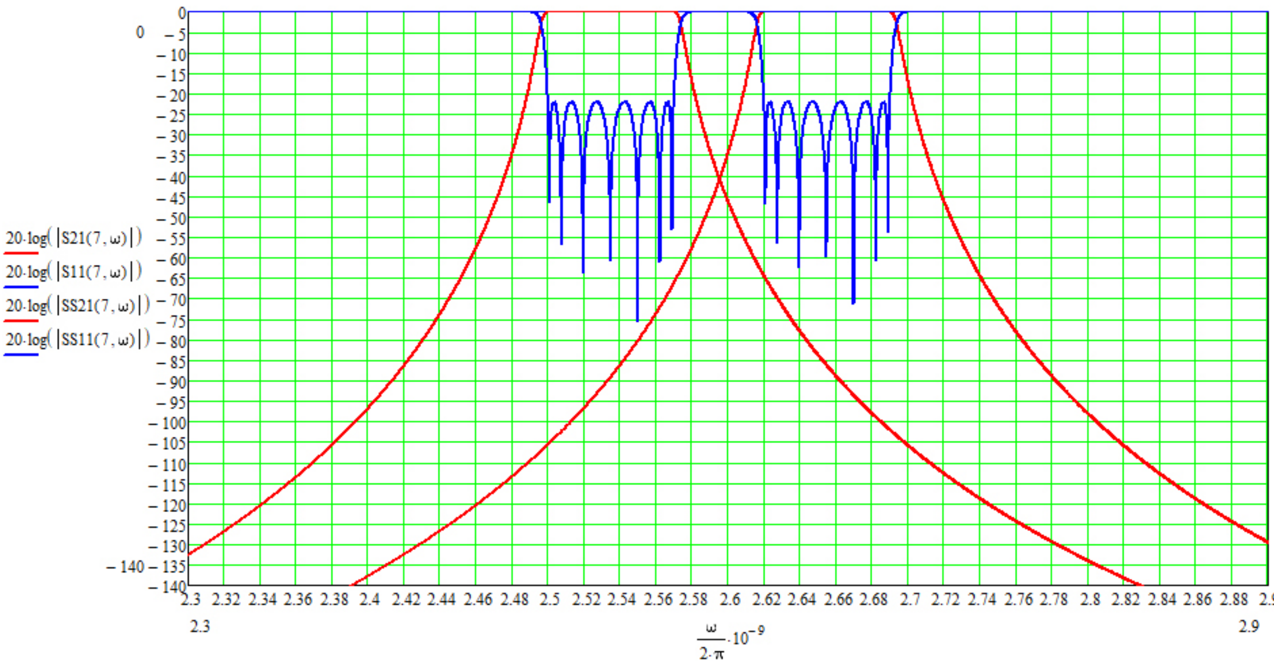

b

Fig. 9. Coupling matrix and external Q-factors (normalised) (*a*) and transmission and reflection characteristics (*b*) of the standard Chebyshev filter of the seventh order of the Rx and Tx ranges for LR = –22 dB

Рис. 9. Матрица связи и внешние добротности (нормированные) (*а*) и характеристики передачи и отражения (*б*) стандартного фильтра Чебышева седьмого порядка Rx и Tx диапазонов для L_R = –22 дБ

(2) Synthesis of the coupling matrix based on the obtained polynomials.

(3) The similarity or rotation matrix transformation method for reconfiguring the coupling matrix into a new one corresponding to the practical topology. Implementation of the initial coupling matrix obtained in step (2) would be difficult because all possible couplings are present (the entire matrix is filled with non-zero elements). The key point of this synthesis method is to reconfigure the obtained initial connection matrix into a matrix with fewer non-zero elements related to the filter topology by a set of matrix rotations. The rotated matrix has exactly the same filter characteristics as the initial matrix.

Synthesis method using optimisation

The second method of synthesising the connection matrix is based on optimisation methods [24]. The principle of optimisation is to minimise the objective function Ω by changing the values of all non-zero elements in the connection matrix.

The objective function Ω is used to quantify the difference between the S-parameters of the current matrix and the expected characteristics of the circuit. Before optimisation, a specific circuit topology is specified. In other words, the locations of non-zero elements in the coupling matrix are determined at the very beginning.

Comparison of two synthesis methods

The first synthesis method, which involves matrix rotation, is very useful. With the help of computers, the initial coupling matrix can be easily found in a recursive manner. However, the matrix rotation methods used to reconfigure the initial coupling matrix cannot solve all problems. Many practical topologies cannot be generated by matrix rotation. It is difficult to determine the sequence of rotation angles to guarantee the convergence of the rotation result. In

$$M3 = \begin{pmatrix} -0.062 & 0.903 & 0 & 0 & 0 & 0 & 0 \\ 0.903 & -0.048 & 0.63 & 0 & 0 & 0 & 0 \\ 0 & 0.63 & -0.049 & 0.568 & -0.145 & 0 & 0 \\ 0 & 0 & 0.568 & 0.228 & 0.572 & 0 & 0 \\ 0 & 0 & -0.145 & 0.572 & -0.053 & 0.633 & 0 \\ 0 & 0 & 0 & 0 & 0.633 & -0.054 & 0.908 \\ 0 & 0 & 0 & 0 & 0 & 0.908 & -0.051 \end{pmatrix}.$$

a

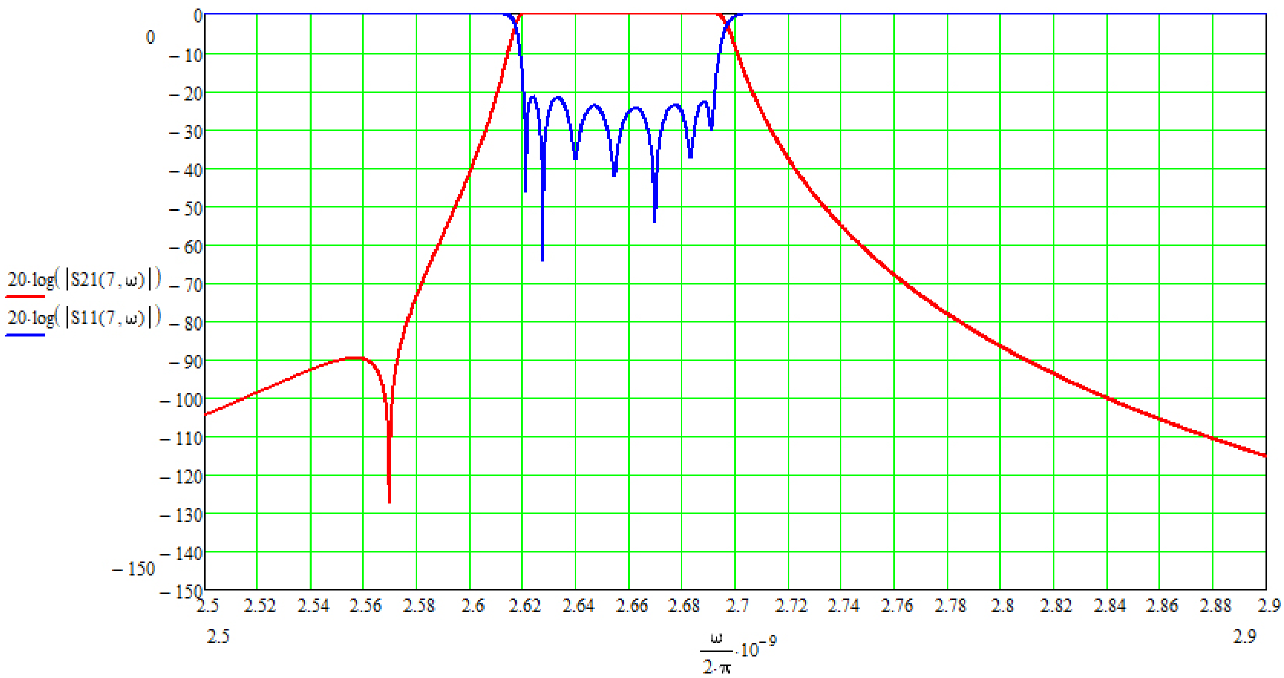

b

Fig. 10. Coupling matrix (*a*) and transmission and reflection characteristics (*b*) of a 7th-order Tx filter with a single cross-coupling
Рис. 10. Матрица связи (*а*) и характеристики передачи и отражения (*б*) фильтра Tx 7-го порядка с одной перекрестной связью

practice, for a given topology limited by manufacturing or application requirements, a connection matrix synthesised by optimisation is still important for designing microwave filters.

Two categories of optimisation methods can be used to synthesise the connection matrix through optimisation. The first is called global optimisation. In global optimisation, the initial point values have little effect on the final result and the total calculation time. This optimisation method searches for the global optimum with the lowest target function values at the cost of low convergence efficiency.

The other optimization method is based on the technique of local optimization. It requires less computation time than the global method. However, the initial approximation is crucial, otherwise the process may converge to a suboptimal local minimum.

4. Construction of a Connection Matrix Using the Local Optimisation Method

As an initial approximation, we take the connection matrix of a filter with standard characteristics, whose connection matrix is determined analytically. When forming the objective function, some critical characteristic points are selected, including reflection zeros *RZ*, transmission zeros *TZ*, passband edges with equal ripple *BE*, and reflection poles in the passband *RP*. As a result, the objective function *CF* in this work is defined as follows:

$$CF = \sum_{i=1}^{n} a_i \left|S_{11}(\Omega_{RZi})\right| + \sum_{i=1}^{4} b_i \left\|S_{11}(\Omega_{BEi})\right| - \varepsilon\right| +$$

$$+ \sum_{i=1}^{n-1} c_i \left\|S_{11}(\Omega_{RPi})\right| - \varepsilon\right| + \sum_{i=1}^{T_2} d_i \left|S_{21}(\Omega_{T_2 Zi})\right|,$$

$$\mathrm{M3} = \begin{pmatrix} 0.055 & 0.939 & 0 & 0 & 0 & 0 & 0 \\ 0.939 & 0.041 & 0.634 & 0 & 0 & 0 & 0 \\ 0 & 0.634 & 0.038 & 0.567 & 0.145 & 0 & 0 \\ 0 & 0 & 0.567 & -0.239 & 0.567 & 0 & 0 \\ 0 & 0 & 0.145 & 0.567 & 0.036 & 0.634 & 0 \\ 0 & 0 & 0 & 0 & 0.634 & 0.037 & 0.938 \\ 0 & 0 & 0 & 0 & 0 & 0.938 & 0.048 \end{pmatrix}$$

a

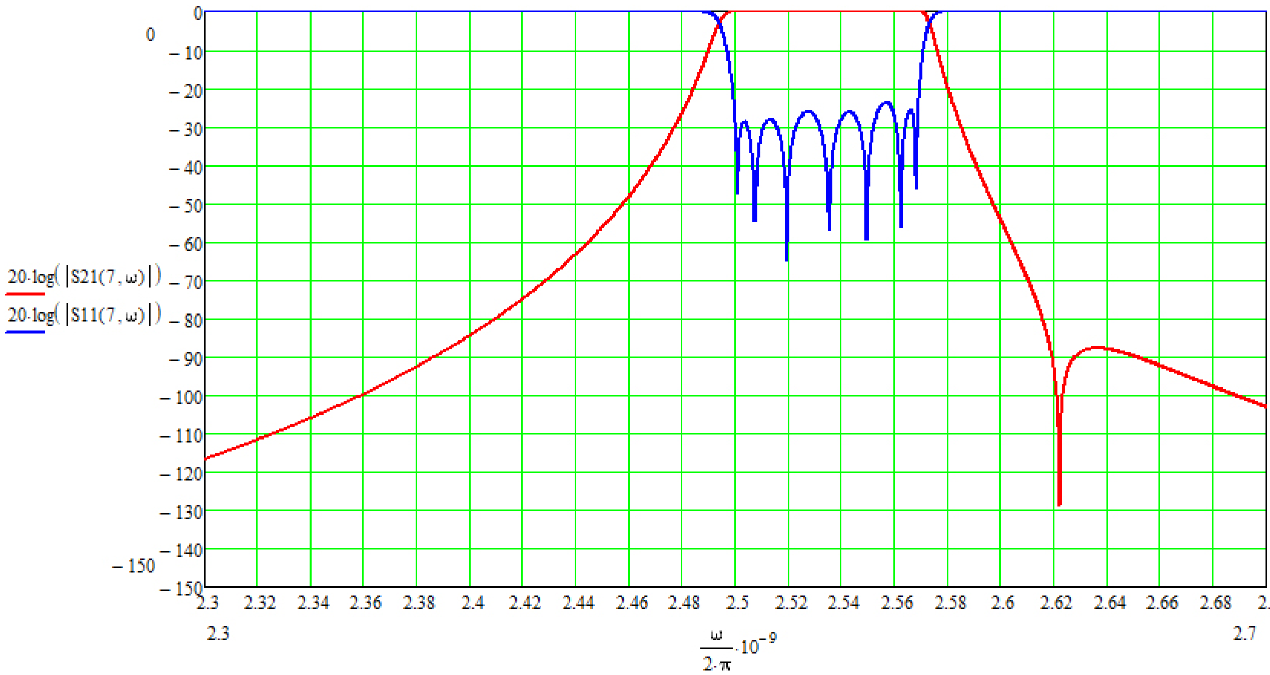

b

Fig. 11. Coupling matrix (*a*) and transmission and reflection characteristics (*b*) of a 7th-order Rx filter with a single cross-coupling
Рис. 11. Матрица связи (*а*) и характеристики передачи и отражения (*б*) фильтра Rx 7-го порядка с одной перекрестной связью

where a_i, b_i, c_i, d_i and e_i are the weights of each term; n is the number of resonators in the circuit; ε is the maximum value of reverse losses in the passband.

The coupling matrix and external Q factors (normalised) of a standard seventh-order Chebyshev filter Rx and Tx ranges for L_R = –22 dB are shown in Fig. 9*a*, and the corresponding characteristics are shown in Fig. 9*b*.

It is possible to improve the characteristics without increasing the order of the filter by creating transmission zeros at the desired frequencies. To do this, additional, so-called cross-couplings, are introduced between non-adjacent resonators. The result of introducing negative coupling between the 3rd and 5th resonators in a 7th-order filter is shown in Fig. 10.

The result of introducing positive coupling between the 3rd and 5th resonators in a 7th-order filter is shown in Fig. 11

As can be seen from the graphs, the attenuation in the adjacent band increased by 25 dB. Further improvement can be achieved by creating another transmission zero.

Fig. 12 *a* and *b* show the characteristics of filters with two additional links between the 1st and 3rd resonators and between the 3rd and 5th resonators. In this case, two transmission zeros are formed in the adjacent band, which allows for an attenuation of -100 dB in a 7th-order filter.

Further improvement of the characteristics requires an increase in the order of the filter.

5. Computer Modelling of Filters

At the initial stage of modelling a multi-link coaxial bandpass filter in CAD, it makes sense to start modelling by studying a filter with one resonator, and then, gradually adding one resonator at a time, evaluate the effect of geometric dimensions on the filter characteristics (S-parameters).

When modelling the filter, the dimensions of the resonators, resonator screws and inter-resonator transitions were specified. When placing the reso-

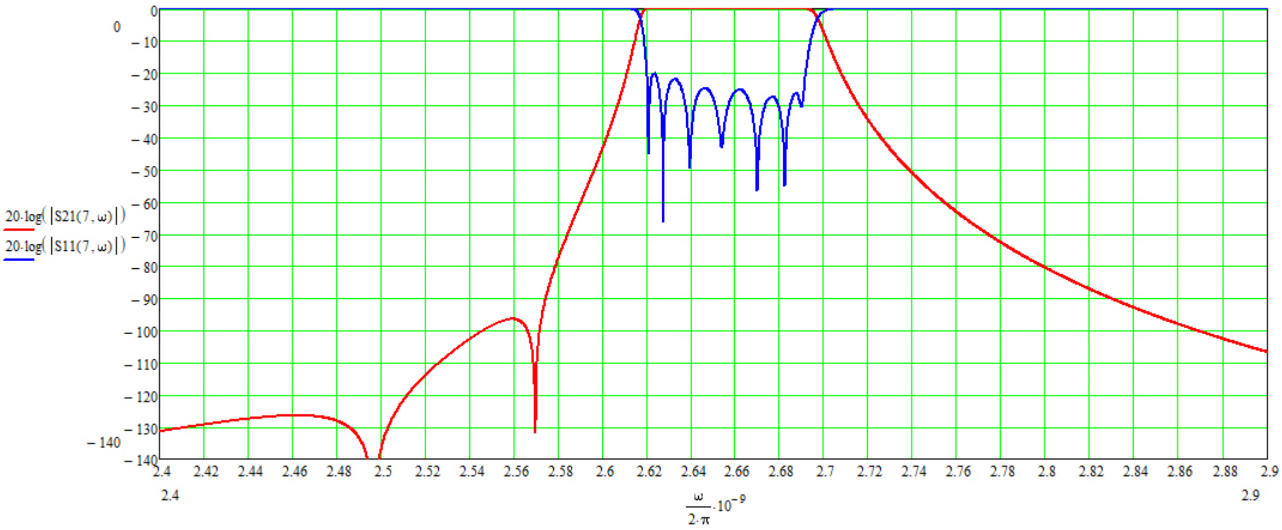

a

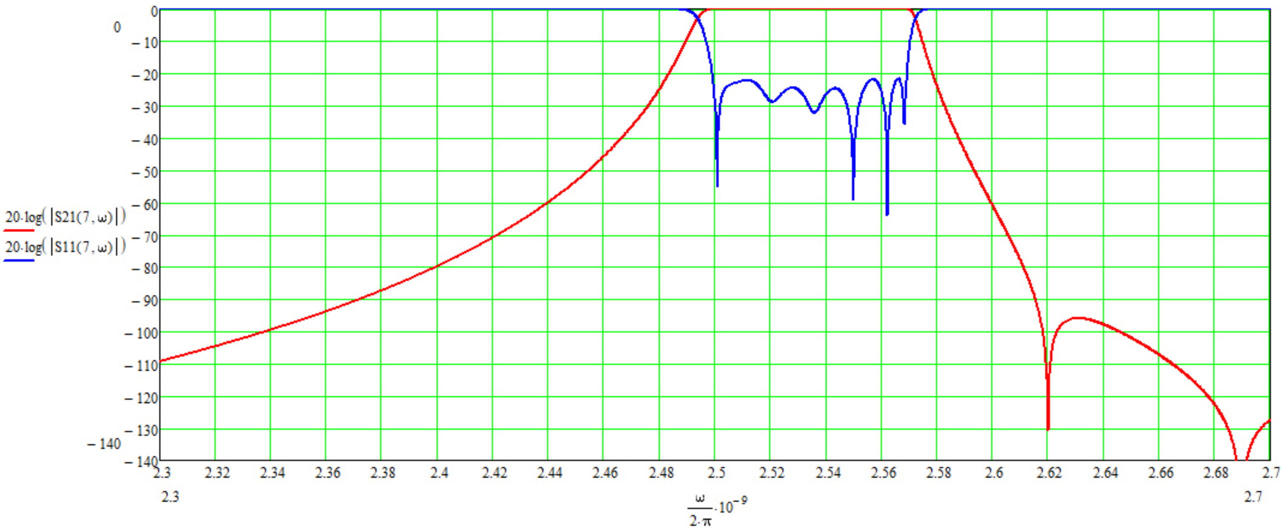

b

Fig. 12. Transmission and reflection characteristics of the Tx (*a*) and Rx (*b*) filters of the 7th order with two cross-links
Рис. 12. Характеристики передачи и отражения фильтров Tx (*а*) и Rx (*б*) 7-го порядка с двумя перекрестными связями

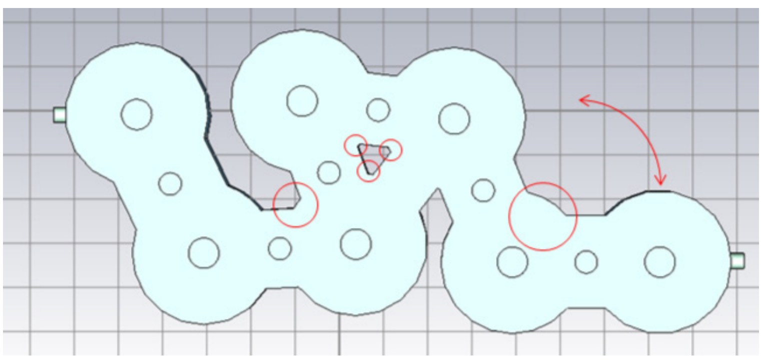

Fig. 13. An approximate filter model
Рис. 13. Примерная модель фильтра

nators, the main goal was to achieve a compact design while taking into account that the dimensions of the inter-resonator transitions would be optimised (Fig. 13).

The modelling was performed using the CST Studio software package. The necessary filter characteristics are achieved using adjustment screws located in the resonator and resonator transitions. The parameters to be optimised were specified in the CAD system. To improve convergence, the aperture of the resonator transitions was included in the list of optimisation parameters. After the model was constructed, the first calculation of the characteristics was performed. Using the built-in CST Filter Designer 3D tool, the matrices of the ideal characteristics and the resulting characteristics were compared.

After starting the optimisation process, the range of parameter changes was reviewed, as their values may exceed the permissible limits. The process will be completed when the convergence function accepts the lowest result.

Conclusion

This paper discusses the principles of constructing filters based on coupled coaxial resonators. Methods for obtaining a given form of the amplitude-frequency characteristic of the filter are analysed using the equivalent circuit method. The principles of calculation and synthesis of filters using connection matrices are described. A method for designing transfer functions and synthesising prototypes of filter circuits with Chebyshev characteristics is considered.

References

1. A. S. Koygerov et al., “Passive bandpass filters for modern microwave communication systems,” Physics of Wave Processes and Radio Systems, vol. 27, no. 1, pp. 71–88, 2024, DOI: https://doi.org/10.18469/1810-3189.2024.27.1.71-88
2. V. A. Kozlov, A. L. Kunilov, and M. M. Ivoylova, “Current state and development prospects of design and technology of ceramic filters for on-board microwave equipment,” Physics of Wave Processes and Radio Systems, vol. 22, no. 4, pp. 61–67, 2019, DOI: https://doi.org/10.18469/1810-3189.2019.22.4.61-67
3. G. L. Matthaei, L. Young, and E. M. T. Jones, Microwave Filters, Impedance-Matching Networks, and Coupling Structures, English trans. by eds. L. V. Alekseev and F. V. Kushnir. Moscow: Svyaz’, 1972, 496 p.
4. J. P. Venter, R. Maharaj, and T. Stander, “Additive manufacturing of interdigital filters with arbitrary line cross section,” *IEEE Transactions on Components, Packaging and Manufacturing Technology*, vol. 10, no. 4, pp. 686–693, 2020, DOI: https://doi.org/10.1109/TCPMT.2020.2967807.
5. J. Li et al., “A Ku-band wideband 3-D printed interdigital bandpass filter free of post fabrication tuning,” 2018 *IEEE International Symposium on Antennas and Propagation & USNC/URSI National Radio Science Meeting*, pp. 1439–1440, 2018, DOI: https://doi.org/10.1109/APUSNCURSINRSM.2018.8608540.
6. Z.-C. Zhang et al., “Triple-mode dielectric-loaded cylindrical cavity diplexer using novel packaging technique for LTE base-station applications,” *IEEE Transactions on Components, Packaging and Manufacturing Technology*, vol. 6, no. 3, pp. 383–389, 2016, DOI: https://doi.org/10.1109/TCPMT.2016.2516820.
7. L. Pelliccia et al., “Compact waveguide bandpass filters for broadband space applications in C and Ku-bands,” 2019 *European Microwave Conference in Central Europe* (*EuMCE*), pp. 116–119, 2019, url: https://ieeexplore.ieee.org/document/8874768.
8. R. J. Cameron, C. M. Kudsia, and R. R. Mansour, *Microwave Filters for Communication Systems: Fundamentals, Design and Applications*. Hoboken: Wiley, 2018.
9. R. R. Mansour, “RF filters and diplexers for wireless system applications: state of the art and trends,” *Radio and Wireless Conference,* 2003*. RAWCON ‘*03*. Proceedings*, pp. 373–376, 2003, DOI: https://doi.org/10.1109/RAWCON.2003.1227970.
10. I. C. Hunter et al., “Microwave filters—applications and technology,” *IEEE Transactions on Microwave Theory and Techniques*, vol. 50, no. 3, pp. 794–805, 2002, DOI: https://doi.org/10.1109/22.989963.
11. G. C. Temes and S. K. Mitra, *Modern Filter Theory and Design*. New York: Wiley, 1973.
12. J. D. Rhodes, *Theory of Electrical Filters*. New York: Wiley, 1976.
13. J. Helszajn, *Synthesis of Lumped Element, Distributed and Planar Filters*. London: McGraw-Hill, 1990.
14. S. Darlington, “Synthesis of reactance-four-poles which produce prescribed insertion loss characteristics,” *Journal of Mathematics and Physics*, vol. 18, no. 1–4, pp. 257–353, 1939, DOI: https://doi.org/10.1002/SAPM1939181257.
15. R. Saal and E. Ulbrich, “On the design of filters by synthesis,” *IRE Transactions on Circuit Theory*, vol. 5, no. 4, pp. 284–327, 1958, DOI: https://doi.org/10.1109/TCT.1958.1086481.
16. G. L. Matthaei, L. Young, and E. M. T. Jones, *Microwave Filters, Impedance-Matching Networks, and Coupling Structures*. Norwood: Artech House, 1980.

17. R. Saal, “Der Entwurf von Filtern mit Hilfe des Kataloges normierter Tiefpässe,” *Frequenz*, vol. 15, no. 4, pp. 111–121, 1961, DOI: https:// doi.org/10.1515/FREQ.1961.15.4.111.

18. J. S. Hong and M. J. Lancaster, *Microstrip Filters for RF/Microwave Applications*. New York: Wiley, 2001.

19. W. Xia, “Diplexers and multiplexers design by using coupling matrix optimisation,” Ph.D. dissertation, the University of Birmingham, 2015.

20. A. E. Atia and A. E. Williams, “New types of bandpass filters for satellite transponders,” *COMSAT Technical Review*, vol. 1, no. 1, pp. 21–43, 1971.

21. A. E. Atia and A. E. Williams, “Narrow-bandpass waveguide filters,” *IEEE Transactions on Microwave Theory and Techniques*, vol. 20, no. 4, pp. 258–265, 1972, DOI: https://doi.org/10.1109/TMTT.1972.1127732.

22. A. E. Atia, A. E. Williams, and R. W. Newcomb, “Narrow-band multiple-coupled cavity synthesis,” *IEEE Transactions on Circuits and Systems*, vol. 21, no. 5, pp. 649–655, 1974, DOI: https://doi.org/10.1109/TCS.1974.1083913.

23. R. J. Cameron, “General coupling matrix synthesis methods for Chebyshev filtering functions,” *IEEE Transactions on Microwave Theory and Techniques*, vol. 47, no. 4, pp. 433–442, 1999, DOI: https://doi.org/10.1109/22.754877.

24. R. J. Cameron, “Advanced coupling matrix synthesis techniques for microwave filters,” *IEEE Transactions on Microwave Theory and Techniques*, vol. 51, no. 1, pp. 1–10, 2003, DOI: https://doi.org/10.1109/TMTT.2002.806937.

Information about the Authors

Yurii G. Belov, Doctor of Technical Sciences, Professor, Department of Physics and Technology of Optical Communication, Nizhny Novgorod State Technical University named after R.E. Alekseev, Nizhny Novgorod, Russia.
Research interests: applied electrodynamics of microwave and HF.
E-mail: bel266@nntu.ru
SPIN code (eLibrary): 7161-8890
AuthorID (eLibrary): 272319

Vladimir V. Biryukov, Doctor of Technical Sciences, Professor, Department of Physics and Technology of Optical Communication, Nizhny Novgorod State Technical University named after R.E. Alekseev, Nizhny Novgorod, Russia.
Research interests: applied electrodynamics of microwave and HF.
E-mail: birukovvv@mail.ru
ORCID: https://orcid.org/0000-0002-6003-0450
SPIN code (eLibrary): 4001-1185
AuthorID (eLibrary): 627885
ResearcherID (WoS): F-3207-2018

Ilya A. Vorobyov, postgraduate student of the Department of Physics and Technology of Optical Communication, Nizhny Novgorod State Technical University named after R.E. Alekseev, Nizhny Novgorod, Russia.
Research interests: applied electrodynamics of microwave and HF.
E-mail: unihoc50@yandex.ru
ORCID: https://orcid.org/0009-0009-6639-6494

Vasiliy A. Malakhov, Doctor of Technical Sciences, professor of the Department of Physics and Technology of Optical Communication, Nizhny Novgorod State Technical University named after R.E. Alekseev, Nizhny Novgorod, Russia.
Research interests: applied electrodynamics of microwave and HF.
E-mail: mr.vasmal@mail.ru
SPIN-code (eLibrary): 6865-6665
AuthorID (eLibrary): 375268
ResearcherID (WoS): E-5392-2014

Aleksey S. Raevskiy, Doctor of Physical and Mathematical Sciences, Head of the Department of Physics and Technology of Optical Communication, Nizhny Novgorod State Technical University named after R.E. Alekseev, Nizhny Novgorod, Russia.
Research interests: applied electrodynamics of the microwave, HF and optical ranges.
E-mail: raevsky_as@mail.ru
ORCID: https://orcid.org/0000-0001-8678-0949
SPIN-code (eLibrary): 1787-5506
AuthorID (eLibrary): 163018
ResearcherID (WoS): E-6791-2014

Yuliya V. Raevskaya, Candidate of Technical Sciences, Associate Professor, Department of Physics and Technology of Optical Communication, Nizhny Novgorod State Technical University named after R.E. Alekseev, Nizhny Novgorod, Russia.
Research interests: applied electrodynamics of microwave and HF.
E-mail: raevskaja.julija@yandex.ru
ORCID: https://orcid.org/0009-0008-2357-2251
SPIN-code (eLibrary): 5101-0265
AuthorID (eLibrary): 627841
ResearcherID (WoS): AAD-3531-2020

Физика волновых процессов и радиотехнические системы
2025. Т. 28, № 1. С. 39–55

DOI 10.18469/1810-3189.2025.28.1.39-55
УДК 621.372.543.2
Оригинальное исследование

Дата поступления 4 ноября 2024
Дата принятия 5 декабря 2024
Дата публикации 31 марта 2025

Методы проектирования полосовых фильтров на связанных коаксиальных резонаторах

Ю.Г. Белов, В.В. Бирюков, И.А. Воробьев, В.А. Малахов, А.С. Раевский, Ю.В. Раевская

Нижегородский государственный технический университет имени Р.Е. Алексеева
603950, Россия, г. Нижний Новгород,
ул. Минина, 24

Аннотация – **Обоснование.** Сверхвысокочастотные полосно-пропускающие фильтры находят широкое применение в различных радиотехнических устройствах. Особое место среди СВЧ полосно-пропускающих фильтров занимают фильтры, входящие в состав мультиплексоров, в частности диплексеров, используемых в системах сотовой связи. В системах мобильной связи широко задействованы конструкции фильтров и диплексеров на коаксиальных резонаторах. Фильтры на коаксиальных резонаторах имеют достаточно хорошо отработанную конструкцию и могут применяться для широкополосных систем. **Цель.** В настоящее время продолжается совершенствование конструкций фильтров и диплексеров на коаксиальных резонаторах с точки зрения совершенствования технологии изготовления и сборки. **Методы.** Метод эквивалентных схем, матрицы связи. **Результаты.** Рассмотрены принципы построения фильтров на связанных коаксиальных резонаторах. Проанализированы способы получения заданной формы амплитудно-частотной характеристики фильтра. **Заключение.** Рассмотрен метод для проектирования передаточных функций и синтеза прототипов фильтрующих цепей с чебышевскими характеристиками.

Ключевые слова – полосно-пропускающие фильтры; коаксиальный резонатор; амплитудно-частотная характеристика; матрица связи.

raevsky_as@mail.ru (*Раевский Алексей Сергеевич*)

Список литературы

1. Пассивные полосовые фильтры для современных систем связи СВЧ-диапазона / А.С. Койгеров [и др.] // Физика волновых процессов и радиотехнические системы, 2024. Т. 27, № 1, С. 71–88. DOI: https://doi.org/10.18469/1810-3189.2024.27.1.71-88
2. Козлов В.А., Кунилов А.Л., Ивойлова М.М. Современное состояние и перспективы развития проектирования и технологии керамических фильтров для бортовой СВЧ-аппаратуры // Физика волновых процессов и радиотехнические системы, 2019. Т. 22, № 4, С. 61–67. DOI: https://doi.org/10.18469/1810-3189.2019.22.4.61-67
3. Маттей Д.Л., Янг Л., Джонс Е.М.Т. Фильтры СВЧ, согласующие цепи и цепи связи / пер. с англ. под общ. ред. Л.В. Алексеева и Ф.В. Кушнира. М.: Связь, 1972. 496 с.
4. Venter J.P., Maharaj R., Stander T. Additive manufacturing of interdigital filters with arbitrary line cross section // IEEE Transactions on Components, Packaging and Manufacturing Technology. 2020. Vol. 10, no. 4. P. 686–693. DOI: https://doi.org/10.1109/TCPMT.2020.2967807
5. A Ku-band wideband 3-D printed interdigital bandpass filter free of post fabrication tuning / J. Li [et al.] // 2018 IEEE International Symposium on Antennas and Propagation & USNC/URSI National Radio Science Meeting. 2018. P. 1439–1440. DOI: https://doi.org/10.1109/APUSNCURSINRSM.2018.8608540
6. Triple-mode dielectric-loaded cylindrical cavity diplexer using novel packaging technique for LTE base-station applications / Z.-C. Zhang [et al.] // IEEE Trans. on Components, Packaging and Manufacturing Technology. 2016. Vol. 6, no. 3. P. 383–389. DOI: https://doi.org/10.1109/TCPMT.2016.2516820
7. Compact waveguide bandpass filters for broadband space applications in C and Ku-bands / L. Pelliccia [et al.] // 2019 European Microwave Conference in Central Europe (EuMCE). 2019. P. 116–119. URL: https://ieeexplore.ieee.org/document/8874768
8. Cameron R.J., Kudsia C.M., Mansour R.R. Microwave Filters for Communication Systems: Fundamentals, Design and Applications. Hoboken: Wiley, 2018. 929 p.
9. Mansour R.R. RF filters and diplexers for wireless system applications: state of the art and trends // Radio and Wireless Conference, 2003. RAWCON '03. Proceedings. 2003. P. 373–376. DOI: https://doi.org/10.1109/RAWCON.2003.1227970
10. Microwave filters-applications andtechnology / I.C. Hunter [et al.] // IEEE Transactions on Microwave Theory and Techniques. 2002. Vol. 50, no. 3. P. 794–805. DOI: https://doi.org/10.1109/22.989963

11. Temes G.C., Mitra S.K. Modern Filter Theory and Design. New York: Wiley, 1973. 566 p.
12. Rhodes J.D. Theory of Electrical Filters. New York: Wiley, 1976. 224 p.
13. Helszajn J. Synthesis of Lumped Element, Distributed and Planar Filters. London: McGraw-Hill, 1990. 380 p.
14. Darlington S. Synthesis of reactance-four-poles which produce prescribed insertion loss characteristics // Journal of Mathematics and Physics. 1939. Vol. 18, no. 1–4. P. 257–353. DOI: https://doi.org/10.1002/SAPM1939181257
15. Saal R., Ulbrich E. On the design of filters by synthesis // IRE Transactions on Circuit Theory. 1958. Vol. 5, no. 4. P. 284–327. DOI: https://doi.org/10.1109/TCT.1958.1086481
16. Matthaei G.L., Young L., Jones E.M.T., Microwave Filters, Impedance-Matching Networks, and Coupling Structures. Norwood: Artech House, 1980. 1097 p.
17. Saal R. Der Entwurf von Filtern mit Hilfe des Kataloges normierter Tiefpässe // Frequenz. 1961. Vol. 15, no. 4. P. 111–121. DOI: https://doi.org/10.1515/FREQ.1961.15.4.111
18. Hong J.S., Lancaster M.J. Microstrip Filters for RF/Microwave Applications. New York: Wiley, 2001. 457 p.
19. Xia W. Diplexers and multiplexers design by using coupling matrix optimisation: Ph.D. dissertation. The University of Birmingham, 2015. 194 p.
20. Atia A.E., Williams A.E. New types of bandpass filters for satellite transponders // COMSAT Technical Review. 1971. Vol. 1, no. 1. P. 21–43.
21. Atia A.E., Williams A.E. Narrow-bandpass waveguide filters // IEEE Transactions on Microwave Theory and Techniques. 1972. Vol. 20, no. 4. P. 258–265. DOI: https://doi.org/10.1109/TMTT.1972.1127732
22. Atia A.E., Williams A.E., Newcomb R.W. Narrow-band multiple-coupled cavity synthesis // IEEE Transactions on Circuits and Systems. 1974. Vol. 21, no. 5. P. 649–655. DOI: https://doi.org/10.1109/TCS.1974.1083913
23. Cameron R.J. General coupling matrix synthesis methods for Chebyshev filtering functions // IEEE Transactions on Microwave Theory and Techniques. 1999. Vol. 47, no. 4. P. 433–442. DOI: https://doi.org/10.1109/22.754877
24. Cameron R.J. Advanced coupling matrix synthesis techniques for microwave filters // IEEE Transactions on Microwave Theory and Techniques. 2003. Vol. 51, no. 1. P. 1–10. DOI: https://doi.org/10.1109/TMTT.2002.806937

Информация об авторах

Белов Юрий Георгиевич, доктор технических наук, профессор кафедры физики и техники оптической связи Нижегородского государственного технического университета имени Р.Е. Алексеева, г. Нижний Новгород, Россия.
Область научных интересов: прикладная электродинамика СВЧ и КВЧ.
E-mail: bel266@nntu.ru
SPIN-код (eLibrary): 7161-8890
AuthorID (eLibrary): 272319

Бирюков Владимир Валерьевич, доктор технических наук, профессор кафедры физики и техники оптической связи Нижегородского государственного технического университета имени Р.Е. Алексеева, г. Нижний Новгород, Россия.
Область научных интересов: прикладная электродинамика СВЧ и КВЧ.
E-mail: birukovvv@mail.ru
ORCID: https://orcid.org/0000-0002-6003-0450
SPIN-код (eLibrary): 4001-1185
AuthorID (eLibrary): 627885
ResearcherID (WoS): F-3207-2018

Воробьев Илья Андреевич, аспирант кафедры физики и техники оптической связи Нижегородского государственного технического университета имени Р.Е. Алексеева, г. Нижний Новгород, Россия
Область научных интересов: прикладная электродинамика СВЧ и КВЧ.
E-mail: unihoc50@yandex.ru
ORCID: https://orcid.org/0009-0009-6639-6494

Малахов Василий Алексеевич, доктор технических наук, профессор кафедры физики и техники оптической связи Нижегородского государственного технического университета имени Р.Е. Алексеева, г. Нижний Новгород, Россия.
Область научных интересов: прикладная электродинамика СВЧ и КВЧ.
E-mail: mr.vasmal@mail.ru
SPIN-код (eLibrary): 6865-6665
AuthorID (eLibrary): 375268
ResearcherID (WoS): E-5392-2014

Раевский Алексей Сергеевич, доктор физико-математических наук, заведующий кафедрой кафедры физики и техники оптической связи Нижегородского государственного технического университета имени Р.Е. Алексеева, г. Нижний Новгород, Россия.
Область научных интересов: прикладная электродинамика СВЧ-, КВЧ- и оптического диапазонов.
E-mail: raevsky_as@mail.ru
ORCID: https://orcid.org/0000-0001-8678-0949

SPIN-код (eLibrary): 1787-5506
AuthorID (eLibrary): 163018
ResearcherID (WoS): E-6791-2014

Раевская Юлия Владимировна, кандидат технических наук, доцент кафедры физики и техники оптической связи Нижегородского государственного технического университета имени Р.Е. Алексеева, г. Нижний Новгород, Россия.
Область научных интересов: прикладная электродинамика СВЧ и КВЧ.
E-mail: raevskaja.julija@yandex.ru
ORCID: https://orcid.org/0009-0008-2357-2251
SPIN-код (eLibrary): 5101-0265
AuthorID (eLibrary): 627841
ResearcherID (WoS): AAD-3531-2020